Atmospheric
Measurement
Techniques
Discussions

Retrieval of volcanic SO$_2$ from HIRS/2 using optimal estimation

Georgina M. Miles[1,2], Richard Siddans[2], Roy G. Grainger[1], Alfred J. Prata[1,3], Bradford Fisher[4], Nickolay Krotkov[5], Brian Kerridge[2]

[1]Atmospheric, Oceanic and Planetary Physics, University of Oxford, Oxford, UK
[2]Remote Sensing Group, STFC Rutherford Appleton Laboratory, Harwell Oxford, UK
[3]Nicarnica AS, Lysaker, Norway
[4]Science Systems and Applications, Inc, 10210 Greenbelt Road, Suite 600, Lanham, Maryland, USA
[5]Goddard Space Flight Center, Greenbelt, Maryland, USA

Correspondence to: G. Miles (georgina.miles@stfc.ac.uk)

Abstract. We present an optimal estimation (OE) retrieval scheme for stratospheric sulphur dioxide from the High Resolution Infrared Radiation Sounder 2 (HIRS/2) instruments on the NOAA and MetOp platforms, an infrared radiometer that has been operational since 1979. This algorithm is an improvement upon a previous method based on channel brightness temperature differences developed by Prata et al. (2003), which demonstrated the potential for monitoring volcanic SO$_2$ using HIRS/2. The Prata method is fast but of limited accuracy. This algorithm uses an optimal estimation retrieval approach yielding increased accuracy for only moderate computational cost. This is principally achieved by fitting the column water vapour and accounting for its interference in the retrieval of SO$_2$. A cloud and aerosol model is used to evaluate the sensitivity of the scheme to the presence of ash and water/ice cloud. This identifies that cloud or ash above 6 km limits the accuracy of the water vapour fit, increasing the error in the SO$_2$ estimate. Cloud top height is also retrieved. The scheme is applied to a case study event, the 1991 eruption of Cerro Hudson in Chile. The total erupted mass of SO$_2$ is estimated to be 2300 kT ± 600 kT. This confirms it as one of the largest events since the 1991 eruption of Pinatubo, and of comparable scale to the Northern Hemisphere eruption of Kasatochi in 2008. This retrieval method yields a minimum mass per unit area detection limit of 3 DU, which is slightly less than that for the Total Ozone Mapping Spectrometer (TOMS), the only other instrument capable of monitoring SO$_2$ from 1979–1996. We show an initial comparison to TOMS for part of this eruption, with broadly consistent results. Operating in the infrared (IR), HIRS has the advantage of being able to measure both during the day and at night, and there have frequently been multiple HIRS instruments operated simultaneously for better than daily sampling. If applied to all data from the series of past and future HIRS instruments, this method presents the opportunity to produce a comprehensive and consistent volcanic SO$_2$ timeseries spanning over 40 years.

1 Introduction

Volcanic eruptions are important for climate and climate change. They perturb atmospheric chemistry and radiative transfer. Their signal in climatic records must be accurately quantified before any attribution of climate change to anthropogenic

Atmospheric
Measurement
Techniques
Discussions

sources. Furthermore, by studying the response of the atmosphere to volcanic eruptions in terms of climate sensitivity this can test ideas relating to climate prediction.

The monitoring of volcanic SO_2 emissions, the main precursor to sulphate aerosols, is crucial for accurately characterising total emission estimates but also for understanding plume evolution. Until the mid-1990's, only one principal instrument

5   (the Total Ozone Mapping Spectrometer, TOMS) has been able to observe eruptions for an adequate period to generate something approaching a climate relevant record. The sensitivity of TOMS limits it to detecting only the larger, explosive eruptions rather than effusive ones where material remains predominantly in the troposphere. Satellite instruments that have been used to measure volcanic SO_2 are given in Table 1. From 1996, with the advent of the Global Ozone Monitoring Experiment (GOME) class instruments (UV-vis spectrometers) sufficient spectral resolution (and spatial resolution) has

10   enabled the detection of lower amounts of SO_2 with higher accuracy from increasingly smaller eruptions. This has improved further still with instruments such as the Infrared Atmospheric Sounding Interferometer (IASI), from which SO_2, sulphate aerosol and ash may be derived simultaneously due to its high spectral resolution and broad spectral coverage (Karagulian et al., 2010). Total erupted mass estimates for volcanic eruptions can often differ by greater than 100% between instruments, as a result of sampling, geometry, differences in sensitivity and assumptions that contribute to algorithms, such as plume

15   height. For example, Thomas et al., (2009) present a multi-sensor comparison of the 2005 eruption of Sierra Negra (Galapagos Islands), using concomitant observations by TOMS, OMI and MODIS. They found a wide estimate of total erupted SO_2 calculated from the three instruments, ranging from 60 kT to 1800 kT.

It is still the case that the operational period of these more sensitive, recent instruments is not yet long enough to constitute a

20   climate-relevant record. Here we present the methodology for a relatively fast and accurate volcanic SO_2 detection method for an instrument originally designed to operationally measure water vapour and temperature profiles.

HIRS/2 has the potential to have captured stratospheric emissions from explosive eruptions continuously since 1979, but with significantly higher temporal sampling and greater sensitivity than TOMS. This enables the 35 year volcanic SO_2

25   emission record from satellites to be significantly enhanced, with potential uses for constraining models and examining in detail individual eruptions and plume evolution.

1.1 HIRS/2 Instrument

HIRS/2 is one of three instruments that originally constituted the Television Infrared Observation Satellite (TIrOS) Operational Vertical Sounder (TOVS), designed to provide atmospheric profile measurements of temperature and water

30   vapour structure (Smith et al., 1979). The other TOVS instruments were the Stratospheric Sounding Unit (a radiometer) and the Microwave Sounding Unit (a scanning microwave spectrometer). The TOVS instrument was first launched in 1979 aboard the new NOAA satellites based on the TIROS-N design, and evolved in to the Advanced TOVS (ATOVS) system. Subsequent replacements have been deployed for the last 30 years aboard NOAA satellites (NOAA 6-17) (JPL, 2003), and

Atmospheric
Measurement
Techniques
Open Access
Discussions
EGU

more recently European platforms including most recently MetOp-A and B as HIRS/4. Throughout its deployment there have been at least two instruments (and occasionally three) orbiting simultaneously. HIRS/2 has 19 detector channels in the infrared and one in the visible part of the spectrum for cloud detection during the day. These channels are relatively broad, spanning between 0.1 and 0.5 μm depending upon wavelength. The key instrument parameters are given in Table 2.

5

Two HIRS/2 channels coincide with SO_2 spectral absorption features, these being 7.3 μm (a strong asymmetric stretch vibration band) and 8.6 μm. The precise central wavenumber is dependent upon instrument version, and only HIRS aboard NOAAs 10 and 12 featured an 8.6 μm channel. These channels were originally chosen to be sensitive to water vapour for use in sounding and applying corrections for the CO_2 and window channels. The 8.6 μm channel is also reported to be
10 sensitive to volcanic ash and other aerosols (Kearney and Watson, 2009).

1.2 Previous efforts to retrieve of SO_2 with the HIRS instrument

Prata et al., (2003) demonstrated a method to detect volcanic SO_2 from HIRS, providing the SO_2 perturbation is strong enough, and located above any significant sources of water vapour. It is based on a synthesis of the expected clean atmosphere brightness temperature for the channel, and the observed deviation from it when contaminated by SO_2. This
15 method, hereafter referred to as either the Pratafit method or after Prata et al., (2003), uses a linear interpolation between the brightness temperatures of adjacent channels. It also assumes a fixed height of erupted volcanic SO_2, since theoretically only one piece of information can be obtained from one channel, and column amount is not insensitive to the height of the plume. The technique requires the SO_2 to be located in the upper troposphere/stratosphere, and there is no information about the height of the plume from the instrument itself. This information may be gleaned from other types of observations, but the fit
20 is reliant upon the accuracy of this independent information.

A description of how the Prata method operates is detailed in Prata et al., (2003). While useful in itself, its most significant shortcoming is that due to its simplicity, the model is unable to capture atmospheric variability (other than potentially that of SO_2). This particularly alludes to the variability of cloud, temperature and water vapour. Without independent height
25 information of the SO_2 the radiance relationships are subject to potentially significant error. Its strengths are that the operations required are computationally inexpensive and straightforward, as it is based on the principles of a band model. It has also performed well against other observational data sets, although the previously mentioned uncertainties that contribute to error make quantifying overall uncertainty difficult. It uses a minimum offset threshold in brightness temperature for the channel affected by SO_2 in order to predict the presence of SO_2 and yet excludes the effects of atmospheric water vapour
30 variability. As such, its sensitivity to low amounts of SO2 is limited.

Guo et al. (2004) presented a re-evaluation of the 1991 Pinatubo eruption using SO2 derived from HIRS/2 using the Prata-fit method, and compared it to SO2 derived from TOMS measurements. They were found to be broadly consistent. The Prata-

Atmospheric
Measurement
Techniques
Discussions

fit method works sufficiently well to suggest that the 7.3 µm SO$_2$ feature it uses is robust enough to make further exploitation more refined. Use of information arising from other HIRS channels would constitute an improvement to the Prata fit method, as multiple wavelength information can be used to diagnose attributes of the atmospheric profile such as temperature and the presence of cloud. This problem is well suited to an optimal estimation retrieval, which would

5   incorporate a forward model (FM) of sufficient complexity to represent these atmospheric attributes. As with the Prata fit, unavoidably it will require some estimate of the altitude of an SO$_2$ plume.

1.3 Outline of paper

In Section 2, an Optimal Estimation (OE) retrieval algorithm methodology to extend the Prata-fit method is presented.

10   Section 3 comprises an error study and presents results of retrievals from simulated measurements in order to understand the sensitivity of the algorithm and potential sources of error. Section 4 presents a case study of the 1991 Cerro Hudson eruption, where the algorithm is applied to real data and new eruption mass estimates are evaluated, and compared to existing mass estimates from other instruments/methods. In Section 5 the results are discussed and further work is suggested.

15   **2 Methodology**

2.1 Retrieval algorithm and forward model

The HIRS/2 measurements used here are all-sky brightness temperatures from NOAA 11. They are a product derived from the raw voltage measurements via a radiance and brightness temperature conversion and have been subject to calibration factors and some basic quality control. The data format contains the time in seconds from midnight of the measurement, the

20   solar zenith angle, 19 IR channel brightness temperatures, one visible channel albedo, latitude, longitude, satellite altitude, line number for each orbit and the scan position (see Table 1).

The retrieval uses three HIRS/2 channels to derive three products: the SO$_2$ column, a scaling factor for a water vapour profile and effective cloud top pressure. The 7.3 µm channel is sensitive to both water vapour and SO2. The weighting function for

25   water vapour of the 6.8 µm channel peaks at around 500 hPa (around 5 km), and as such would have some sensitivity to the region where the vast majority of the water vapour in the column resides. To represent both channels accurately, some knowledge of cloud is required, which may be gleaned from the 11.1 µm channel window channel. This channel is highly sensitive to the emitting temperature of the lowest surface it observes (be it cloud or the surface), thus with some knowledge of the surface and atmospheric temperature profile it is possible to obtain an estimate of cloud top height.

30

Atmospheric
Measurement
Techniques
Open Access
EGU
Discussions

Radiative Transfer for TOVS (RTTOV) is a radiative transfer model (developed by the UK Met Office, Saunders et al., 1999, ECMWF 2001) designed to simulate the instruments of TOVS including HIRS/2, and is used extensively (particularly for assimilation) because of its speed. It calculates layer transmittances for a variety of trace gas species using look-up tables of parameterised regression coefficients for a range of temperatures and pressures. It has been further developed since the

5   TOVS system was first deployed, and version 10 is used here. RTTOV also has the functionality to compute partial derivatives.

RTTOV estimates channel brightness temperature based on pre-calculated coefficients for layer transmittances that are generated for a range of atmospheric profiles. As such, it is extremely fast, but as it stands it does not incorporate any

10   representation of SO_2 other than at a very low climatological value. To alter the transmittance model to include SO_2 would require substantial re-working of program code. It is possible to calculate a set of predictor coefficients for SO_2 and incorporate them within RTTOV by replacing the properties of another gaseous species that has negligible impact on the total column transmittance within the selected HIRS/2 channels (in this case, carbon monoxide). The coefficients were generated by a `training' methodology using an extensive range of specimen atmospheric profiles, where the SO_2 was

15   represented from very low/background levels to very large perturbations, after Matricardi (2008, 2010) and Siddans (2011). This approach retains the speed and accuracy offered by RTTOV and enables the model to be used to represent atmospheric gases for future instruments not already catered for (ECMWF, 2001).

For this work, the predictors were trained using profiles with up to 300 DU. Some care is required in the generation of these

20   coefficients for SO_2. They are required to be limited to those that represent a first order relationship with SO_2 since the more complicated (higher order) predictors caused erroneous results. This is thought to be a result of both the dynamic range SO_2 can exhibit in a volcanically perturbed atmosphere, and the fact that RTTOV was not explicitly designed to model SO_2 for this instrument. The cost in terms of accuracy over this range of SO_2 is shown to be small up to the training limit (see Fig. 1).

25

The column retrieval developed here uses atmospheric profiles from the ECMWF ERA-Interim product (Dee et al., 2011) to represent atmospheric properties other than SO_2, or as a first guess in terms of the water vapour profile. These contain profiles on a pressure grid of 37 levels from 1000 hPa to 1 hPa. RTTOV is capable of generating weighting functions, but they refer to the sensitivity of the simulated measurements to perturbations in the atmospheric profile, rather than directly to

30   changes in state vector. As a result, these are calculated numerically in the forward model. RTTOV has certain physical limits for its input values, and when occasionally the predicted updated state lies outside these they are manually constrained in the FM by the physical limits that RTTOV will accept. The weighting functions are allowed to make linear extrapolations beyond these limits, allowing the retrieval more freedom, but unphysical profiles are suppressed with quality control of the derived products (discussed later).

2.2 Profile definition in forward model

The three-element state vector comprises a scaling factor for the SO_2 profile, a scaling factor for a water vapour profile and a
5   cloud top pressure. A volcanic SO_2 perturbation is represented by a vertically localised triangular profile. This triangular
profile is normalised to have an integrated mass of 1 DU. This was partly done to ease interpretation, since the retrieved
scaling factor would be approximately equal to the total amount of SO_2 in the column. The rest of the profile is prescribed
by a background SO_2 volume mixing ratio climatology, the total column mass of which is less than 1 DU. In the forward
model, a scaling factor applies to a specified height region of the SO_2 profile, scaling all elements within and none outside
10   this. The expected region of the volcanic plume is estimated using ancillary information, such as lidar or results from
modelling of the eruption available in the literature. The sensitivity to how well the altitude and thickness of an SO_2 plume is
evaluated using retrievals from simulated measurements, and detailed in Section 3.

In an analogous way to SO_2, H_2O is represented in the state vector by a profile scaling factor, but it applies to the entire
profile rather than a localised height region. The profiles used for retrieval are those collocated from the ECMWF ERA-
15   Interim product for a given HIRS/2 pixel (which represents the best guess for the state), but in principle any climatological
profile can be used. In the case where a scaling factor is close to one, it would indicate that the H_2O profile is similar to that
which produced the measurement.

The third element of the state vector is cloud top height (CTH), or specifically the geopotential height at an equivalent
pressure level. It was found that the speed of convergence was significantly reduced if the initial guess of cloud top pressure
20   was reasonably accurate. As such, this is derived before the retrieval using interpolation between calls to a radiative transfer
model that simulates the 11.1 μm channel brightness temperature (BT) for 0-10 km (using associated ECMWF ERA Interim
temperature profile), and included a test for temperature inversions.

2.3 Error

An estimate of forward model error was calculated using the Reference Forward Model (RFM) — a line-by-line radiative
25   transfer model (Dudhia, 2002), discussed further in Section 3. The estimate accounts for inaccuracies that arise due to
modelling the atmosphere at reduced spectral resolution, limited vertical resolution, inclusion of non-retrieved trace gases at
a climatological level or their preclusion entirely, relative to a reference case. This yields a channel quantity (in brightness
temperature) that is combined in quadrature with the noise equivalent differential radiance for each channel, and is thus
incorporated into measurement noise for the purposes of the retrieval. The a priori error associated with cloud height is 10
30   km.

2.4 Estimation of SO₂ and H₂O covariance for HIRS/2

Establishing an appropriate SO_2 a priori error is potentially a non-trivial issue with regard to a retrieval problem where the measurements have relatively little sensitivity. A volcanically perturbed SO_2 profile can contain 2 or 3 orders in magnitude more than a background profile, and at the centre of a large plume this can be even more. A good a priori error gives the

5   retrieval the freedom to find a correct minimum in cost space, and can restrict it from converging on a solution that is unphysical. The variance for a background profile would be very small, as opposed to a profile where SO_2 is expected, which would be very large. If there is sufficient information contained within the measurements, one would conventionally use a variance that spans both scenarios. This results in a poor constraint for an ill posed problem but is necessarily used here, where a first guess/a priori error of 100 DU is used and a prior variance is the first guess squared.

10

Early results of the retrieval scheme run with real measurements revealed that there were many `false positives' of SO_2 retrieved. Their structure indicated that they were related to the presence of water vapour, or errors in the fit for water vapour. This indicated the degree of covariance between SO_2 and water vapour which had to be incorporated into the retrieval since the 7.3 μm channel is sensitive to both water vapour and SO_2.

15

The retrieval was applied to one day of `clean' measurements in the Southern Hemisphere where no volcanically perturbed profiles were expected. The retrieval was forced not to retrieve SO_2 by artificially constraining the a priori variance, but none-the-less small amounts of SO_2 are retrieved from that channel because of inadequacies in characterising the water vapour. The brightness temperature fit residuals in the SO_2 channel were very small, but it is expected that nearly all of the

20   SO_2 being retrieved on this day is being falsely attributed. The standard deviation of the 7.3 μm channel brightness temperatures fit residual in the retrieval of 0.92 K constitutes an estimate of the 'real world' error covariance of water vapour with SO_2 for this instrument. This is incorporated by adding it in quadrature to the forward model error for this channel and resulted in a significant reduction in the occurrence of false positives.

25 ## 3 Error study: Retrievals from simulated measurements

The main sources of error that cannot be adequately represented in the forward model are errors that impact ill-posed nadir SO_2 column retrievals in general. These are incorrect height assignment of the SO_2 plume, incorrect thickness in the plume represented in the forward model and particularly in the case of infrared measurements and sensitivity to the presence of cloud and/or water vapour. Their relative impacts vary and the sensitivity of the solution to them can be quantified using

30   simulations.

Atmospheric
Measurement
Techniques
Discussions

Open Access

EGU

3.1 Spectral precision of forward model

In order to assess the accuracy of the RTTOV-based fast column retrieval forward model, it is compared to simulations from a model with a higher accuracy. The RFM is a line-by-line radiative transfer model (Dudhia, 2002) capable of modelling the

5   atmosphere at a spectral resolution of up to 0.0001 cm^{-1}. The RFM is not suitable for the forward model because it is computationally expensive and it does not inherently represent any effects of cloud or ash. Figure 1 shows the results of column retrievals from HIRS/2 channel BTs simulated by the RFM, using a sample ERA-Interim cloud-free meteorology (temperature and water vapour profiles) at 0 and 60°S latitude and 0°W longitude, where only the column amount of SO_2 is changed in the simulation. It also shows the SO_2 fit by the Pratafit method. The Pratafit method does not fit SO_2 below 5

10   DU, which depending upon the atmospheric state can be equivalent to an observed brightness temperature difference of up to 4 K. The bias of the Prata fit has a dependence upon latitude, primarily because of the different amount of water vapour in the profile at the two latitudes shown here. The column retrieval has a very small bias that only becomes perceptible at SO_2 loadings approaching 200 DU, at which point it is of the order of <5 DU.

15

3.2 Sensitivity to forward model representation of SO_2 plume

Both the altitude and amount of SO_2 affect the 7.3 μm channel brightness temperature but as there is only one channel sensitive to SO_2 on NOAA11 considered here, there is at most one piece of information that can be retrieved for SO_2. Therefore, for an accurate retrieval of SO_2 column, it is important to have some knowledge of the plume altitude or its

20   vertical profile. The column retrieval developed here requires some information of the height of the SO_2, but this can be subject to uncertainty and may change with time. As such, the sensitivity of the retrieval to errors associated with plume height and specification must be examined.

3.2.1 Altitude

25   Measurements were simulated for a plume at a range of altitudes from 8-18 km. Figure 2 shows the impact on the retrieved SO_2 column at a specified, fixed altitude as a fraction of the true column at these altitudes. This is the largest source of error in the OE column retrieval (and the Prata-fit method) and it is clear therefore that good prior knowledge of the SO_2 plume altitude is necessary for accurate retrieval or fit of SO_2 column amounts from HIRS/2.

The performance of the column fit was also assessed against a line-by-line model (RFM) for plume altitudes from 8 to 18 km and it was found that for altitudes of over 17 km the column fit was unable to retrieve SO_2 columns less than 30 DU, but in all other cases true clear-sky column amounts were retrieved accurately from simulated measurements.

5

3.2.2 Profile shape and plume thickness

Figure 3 shows the consequences that can result from retrieving the volcanic plume with a fixed profile shape that represents the thickness of the plume incorrectly. Measurements were simulated using a triangular profile centred at 12 km but with baselines of 1 and 4 km. They were then used in the retrieval with a fixed profile shape with a triangular perturbation also centred at 12 km, but with a baseline of 2 km (thought to be the best representation of the plume used in the case study in Section 4). The retrieval simulations suggest that errors are larger when the plume thickness is overestimated, with only small inaccuracies introduced when the plume thickness is under-estimated. The modelled cloud top height was 3 km in all cases.

3.3 Sensitivity of Retrieval Scheme to Cloud and Ash

Some understanding must be obtained of how the column retrieval forward model behaves in the presence of ash and cloud of different type. The forward model fits a cloud top pressure using the 11.1 μm channel, which is expected to work well for most scenes with cloud in the troposphere. The effect of cloud on the other channels is examined here using a cloud model, the Oxford-RAL Retrieval of Aerosol and Cloud (ORAC) model. The model is described in detail by Poulsen et al. (2012), where it was used as part of an optimal estimation retrieval of cloud properties for the Along Track Scanning Radiometer (ATSR) by simulating radiances in a combination of visible, near infrared (NIR) and IR channels. The model parameterises a cloudy scene by ascribing cloud phase, effective radius of a size distribution, the 0.55 μm optical depth and a cloud top pressure. It uses the plane parallel approximation and models cloud as a single layer. The model represents trace gases at a background climatological level. The system can also be used to retrieve ash plume properties: plume height, optical thickness and ash particle effective radius (McGarragh et al., in preparation, 2017)

HIRS/2 measurements were simulated for a range of liquid and ice cloud and ash optical depths, effective radii and at a range of altitudes when no volcanic SO_2 is present. These channel brightness temperatures were then used to retrieve SO_2 to identify where this resulted in an erroneous fit.

An example is shown in Fig. 4, which shows that for water vapour clouds above 5 km, the column retrieval erroneously retrieves some SO_2 when there is none, the water vapour and cloud top height become inaccurate and the fit cost begins to increase. The results indicated that low optical depth or effective radii for cloud or aerosol can result in poor fitting of the measurements, both resulting in an underestimate of cloud top pressure with false positives of SO_2 and an over-estimation of

Atmospheric
Measurement
Techniques
Open Access
Discussions
EGU

water vapour. This yields a crucial quality control threshold where retrieved cloud top altitudes of greater than 5-6 km should not be trusted, as they are likely to result in spurious detection of SO_2 and a high retrieval cost. This may imply that very thin cloud beneath 5 km (or incorrectly retrieved to be) could still contribute to poor fitting of the measurements.

5

3.4 Quality Control

The results of the column retrieval must be subject to some quality control. In addition to the disregard of non-converged and converged pixels with cloud retrieved at an altitude greater than 5 km, a retrieved column is only considered useful if the error is less than the retrieved amount. Quality control becomes very important when erupted plumes are used to calculate

10 total erupted mass, where even a small amount of noise can yield a biased mass total. For the purposes of gridding or summing pixels for deriving a global/plume mass estimate, a minimum retrieved SO_2 threshold may be applied in deference to the lower detection limit of the retrieval, in order to avoid spurious low values that the retrieval should not be sensitive to, such as those relating to water vapour or cloud that are not accounted for in either the error covariance or the forward model. An effective way of obtaining this quantitatively is to apply a 2 or 3 sigma test, where sigma is the standard deviation of the

15 retrieved SO_2 on a day when no volcanic SO_2 is expected to be present. This threshold gives statistical confidence that a value above it is significantly distinct from the noise above the 95 or 97 percentile. The sigma threshold for 6th August 1991 (a day when there was no SO_2 present in the region relating to the case study in Section 4) was 2.7 DU, and is probably a lower estimate of the detection limit of the HIRS/2 SO_2 column retrieval in the mid-latitudes. Multiples of this value indicates confidence that a retrieval result is dominated by signal rather than noise.

20

4 Case Study: Cerro Hudson Eruption in 1991

Cerro Hudson (45.54°S, 72.58°W, elevation 1905 m) is a stratovolcano in the south Chilean Andes that erupted explosively in August 1991, two months after the Pinatubo eruption. The eruption was estimated to be 10-20 times smaller than Pinatubo in terms of SO_2 that was expected to be emitted. At the time of the 1991 eruption, the only satellite available that

25 could detect SO_2 with any demonstrated accuracy was TOMS. The Microwave Limb Sounder, a contemporaneous instrument that observed SO2 from Pinatubo at a higher altitude, produced noisy results in the lower stratosphere at this latitude (Read et al, 1993). As well as some ground observations, the Hudson eruption was sensed remotely by AVHRR (ash), lidar (sulphate aerosol) and incidentally by an aircraft (Barton et al. 1992). Hofmann et al. (1992) reported possible

30 exacerbation of Antarctic ozone depletion of 10-20% of total column due to the presence of Hudson aerosol in the lower stratosphere for September 1991. The anomalous depletion occurred within the polar vortex predominantly at 11-13 km and

Atmospheric
Measurement
Techniques
Discussions

25-30 km, the respective altitudes of the Hudson and Pinatubo aerosols. The transport of the Hudson volcanic plume was first numerically modelled by Barton et al. (1992), to reasonably good agreement with satellite and lidar observations. The plume was also modelled using an isentropic trajectory model, initiated by TOMS observations of SO_2 (Schoeberl et al. 1993). These models showed good spatial agreement with observations for the first eight days after the eruption which is an indication that the height assignment of the erupted plume was accurate within the models. The most explosive eruption began and ended on 15th August. It was at this stage of its eruptive phase that the majority of the material was injected into the stratosphere (Constantine et al. 2000).

4.1 Results

Figure 5 shows an example of the SO_2 retrieval applied to a day of data on 15th August 1991, and its associated retrieval error. Figure 6 shows results for the same day as Figure 5, but for the other elements of the state vector: the retrieved water vapour scaling factor and cloud top height (with their associated retrieved errors). Only high cost and convergence criteria have been applied. In general, the retrieved values of cloud top height have very small errors. For the water vapour scaling factor, the largest errors occur in the presence of high or thick cloud, which is expected. As shown in Section 3, the cloud model simulations suggested that the retrieval struggles in the presence of high cloud and can on occasion fit spuriously enhanced SO_2, potentially because it results in a poor estimate of water vapour in the correspondingly colder scene. Regions of very high water vapour scaling factor result in very high errors in retrieved SO_2, and data with cloud top height greater than 5 km are not considered reliable for SO_2.

Figure 7 shows nine days of retrieved SO_2 from the 1991 Cerro Hudson eruption following the largest eruption phase on 15th August. The eruption began on 8th August emitting smaller amounts of SO_2 into the upper troposphere lower stratosphere, which can be seen as already present in the path of the main plume on subsequent days. The multiple sampling of the plume by successive orbits (day and night) is quite apparent, particularly as the plume becomes more distorted after 20th August.

4.2 Plume Mass Estimate

The simplest method to estimate the total erupted mass or mass present in a volcanic plume is to take the sum of the representative footprint areas of the satellite that measured SO_2. This method presents several problems relating to sampling of a volcanic plume, particularly with an infrared instrument that measures both night and day that could sample the plume more than once, orbits may partially sample the plume in any one swath and the plume will move constantly between sampling. Alternatively, gridding averages the data into grid boxes on a latitude and longitude grid. Some care must be taken to account for whether or not the gridded data are representative of the data resolution, and keeping track of bins with no data can be a way to estimate under-sampling. Guo et al. (2004) used two methods of gridding data, that of kriging for TOMS data and nearest neighbour interpolation for HIRS/2 (Pratafit method) to account for larger spatial gaps between points. These methods either impose statistical methods or manually introduce information based on assumptions. While

Atmospheric
Measurement
Techniques
Discussions

both can be utilised in such a way as to indicate an estimate of the error or uncertainty that this introduces, mass estimates presented here are only based on the sum of equivalent contiguous footprints represented by each HIRS ellipse.

Furthermore, if gridding is used, in order to ensure that the data are sampled fairly, the orbits should first be split into
5 ascending and descending nodes, with care taken regarding where a plume is in relation to the date line. This is in an effort to minimise recording the same data point twice when the plume has moved by the time the region is sampled again. Other methods are available but often require a model or further ancillary information.

10 **4.3 Comparative measurements of SO$_2$**

The plume mass estimate for the HIRS/2 SO$_2$ retrievals for the Cerro Hudson eruption may be qualitatively compared to the figures for TOMS within Constantine et al. (2000). Total erupted mass estimates given can be directly compared, as shown in Table 3, although the methodology by which the estimates were derived differs. Spatially, HIRS/2 has the advantage of smaller footprint than that of TOMS, (IFOV 1.25° x 1.25°/17.4 km x 17.4 km verses 3° x 3°/ 50 x 50 km) but the TOMS
15 swath is 50% wider (3000 km). For a case such as the Hudson plume, TOMS is more likely to capture the entire plume in one orbit swath and sample it only once, which on the one hand greatly reduces ambiguity in deriving total plume mass but on the other hand the frequency of observation is reduced and sometimes only part of the plume is captured. As reported by Constantine et al. (2000), this was sometimes the case, and a 'best' estimate of the TOMS data was used to contribute to the values in Table 3.

20

The erupted mass estimates given in Table 3 that relate to HIRS/2 are the sum of equivalent footprint areas , from nodes that capture the most of the SO$_2$ plume present each day. Figures are rounded to reflect probable accuracy. For the total eruptive period, this method has yielded a total erupted SO$_2$ mass estimate of 2300 kT with an averaged retrieved error of 27 %. This error does not incorporate error that arises from uncertainty in the height of the SO$_2$ in the forward modelled plume (as
25 demonstrated in Section 3), or error that might arise from discounting pixels where SO$_2$ was retrieved below the 3-sigma threshold. It does not account for absent scanlines due to instrument calibration, so should be considered a lower limit. As previously discussed, a good estimate of plume height is an unavoidable requirement in SO$_2$ detection with an instrument with only one channel sensitive to atmospheric SO$_2$. In the case of this work, height assignment error of ± 1 km introduces a mass dependent bias of between 5 and 20% for a given pixel depending upon where in the atmosphere the plume is located.
30 For TOMS, the approximate error suggested for the total erupted mass estimate is 30% (Krueger et al, 1995, Constantine et al. 2000).

The TOMS algorithms used in Constantine et al. (2000) have been recently updated, and a brief comparison is presented here to some initial data from an updated TOMS algorithm. This algorithm exploits the way ozone and sulphur dioxide both

strongly absorb UV radiation. The new TOMS algorithm builds on the early heritage of BUV algorithms (Krueger et al., JGR, 1995). These algorithms retrieve both O_3 and SO_2 by taking advantage of the large SO_2/O_3 cross section ratio (CRS) differences in the gas absorbing bands. This approach constructs radiance tables using a forward model that accounts for both the O_3 and SO_2 cross sections. The new algorithm uses the 317 channel to retrieve SO_2 (CRS ~ 2.5), the 331 nm channel

5 to retrieve O3 (CRS ~0.15), and the 340 to retrieve the spectral dependence, dR/dλ. This methodology further applies a small second order step2 correction that accounts for non-orthogonality between the SO_2 and O_3 channels.

A one week composite of retrieved SO_2 for both instruments is shown in Fig. 8 where SO_2 from the main eruptive phase can be seen circumnavigating the hemisphere. There is clear complementarity between the instruments in terms of absolute

10 amount retrieved and characterisation of the plume. The smaller pixel size of HIRS and more frequent sampling enables the plume to be observed in finer detail; however the wider swath of TOMS frequently captures more of the plume in one swath. For a more detailed comparison, two orbits during the 1991 Hudson eruption are considered where the plume is almost fully sampled by both instruments, as shown in Fig. 9. The pixels in the region of the plume were also relatively cloud-free or had low cloud during the observation.

15

The geographical bounds considered for the mass estimate are between -53° and -45° in latitude and 10° to 60° in longitude. Using the method of summing over mass and area discussed previously, the mass of the plume represented here by HIRS/2 and TOMS is calculated to be 1398 and 1540 kT respectively, after quality control has been applied. The missing four scan lines due to a HIRS calibration phase that coincide with the plume in the region of high concentration suggests the HIRS

20 estimate is an underestimate. It is apparent that HIRS/2 is potentially more sensitive to lower amounts of SO_2. It is challenging to directly compare the SO_2 retrieved by two instruments with differing footprint sizes. Gridding might offer an alternative method of plume mass estimate, but selection of the most appropriate grid box size relative to the pixels of each instrument coupled with the small size of the plume with a strong SO_2 concentration gradient make it a challenge for such a comparison to be equitable and account for instrument attributes. A comparison involving gridding for a larger eruption (c.f.

25 Pinatubo) would be less problematic.

4.4 E-folding time

The e-folding time for erupted SO_2 is a measure of the residency of the material in the atmosphere, and is affected by the height the material reaches and in the case of very large eruptions, the amount itself. It is also affected by wind shear

30 (horizontal and vertical) and humidity, which affects the rate at which the SO_2 is oxidised and sulphate aerosols grow. The measure is more suited to large eruptions (e.g. El Chichón in 1982 or Pinatubo in 1991), in terms of inferring effects upon radiative forcing, about which Miles et al. (2004) and other works are concerned. This is because the amount and height that such eruptions reach in the stratosphere gives the SO_2 sufficient time to become globally mixed, and as such affect the

Atmospheric
Measurement
Techniques
Discussions
Open Access
EGU

radiative forcing globally. Equation 1 describes the process of exponential decay, where $N(t)$ is a quantity at time t, N_0 is the initial quantity at time $t=0$ and λ is the decay constant.

$$N(t) = N_0 e^{\lambda t} \tag{1}$$

The e-folding time, the time in which the initial quantity is reduced to $1/e$ of its initial value, is given by the reciprocal of the

5   decay constant. Using approximate values from the mass estimates derived from Fig.8 where the total SO_2 can be said to drop from around 1500 kT (the total mass present on 17th August 1991 associated with main plume) to 500 kT 18 days later, this yields an e-folding time of around 16 days. Two days after the largest plume was erupted is used here to minimise potential obscuration of the plume by the coincident presence of thick ash. The variability of the mass estimates and the associated retrieval error make only an estimate appropriate for this approach, but it is not considered to be an unreasonable

10   one. If the e-folding time is calculated for the extremes of the retrieved error bounds of the mass estimates, the e-folding time is 10 days at a minimum, and 35 days at its shallowest descent, but these are considered to be overly-generous bounds by this method. The e-folding time for this SO_2 plume as estimated by Constantine et al. (2000) is around 15 days, but they state that this is algorithm dependent. These estimates are somewhat smaller than the e-folding times for the larger eruptions (e.g. Pinatubo), which is to be expected due to the considerably lower altitude of the Hudson plume. More recently, Carn et al.

15   (2016) estimated the e-folding time of Cerro Hudson to be ~7 days. They attribute this anomalously short e-folding time to the late southern hemisphere winter timing of the eruption.

5 Discussion

This OE column retrieval finds a new total erupted mass estimate for the 1991 eruption of Cerro Hudson of 2300 ± 600 kT

20   from the HIRS/2 instrument aboard NOAA11. This does not incorporate any error from plume altitude estimation but the potential impact has been quantified by forward model simulations. This total mass estimate is lower than that of TOMS (Constantine et al. 2000) and that of Carn et al. (2016) but higher than that derived in a similar way using the methodology of Prata et al. (2003) for HIRS/2. Reasons for this include (but are not limited to) differences in sampling, height sensitivity, instrument differences and attributes or accuracies of the forward model or fit employed in SO_2 detection. From the

25   comparison with the new TOMS algorithm, the HIRS/2 results presented here are highly consistent, and further quantitative comparison, for this eruption in particular, is desirable.

The retrieval precision demonstrated in this case study is slightly smaller (~3 DU) than that proposed for the TOMS instrument (6-7 DU). As such, with the increased sampling of the IR instrument it is apparent that HIRS/2 can offer a positive contribution to the atmospheric SO_2 emission record from explosive volcanic eruptions up to and beyond the launch

30   of GOME and other satellites that followed. Moreover, benefits of the optimal estimation approach over and above the more rapid but limited brightness temperature difference method are significant. They include a quantified error on individual pixel retrieved values, diagnostic indicators of the retrieval performance and goodness-of-fit and treatment of cloud and

water vapour consistent to the retrieval of SO_2. When summing mass over a large number of pixels, the precision that these afford becomes increasingly important.

There are clear opportunities for extending this work. In particular, as the HIRS/2 instrument was present aboard a number of the NOAA platform series, and often simultaneously flown (NOAA 10, 11 and 12 were all in orbit at the time of the Cerro Hudson eruption) there is the possibility to fully characterise eruptions with very high temporal sampling. More rigorous methods for interpolation, sampling and gridding the data can also be used to reduce errors in the total mass estimates. The application of further tools such as chemistry transport or trajectory models for understanding plume evolution would be better constrained by the availability of more measurements.

The first HIRS instrument was flown aboard TIROS-N in 1978, and there are almost continual data available to the present, and for the foreseeable future of the Met-Op series of satellites, enabling a potential dataset spanning 40+ years. Generating an SO_2 dataset for the duration would be an opportunity to maximise the value and legacy of the satellite data. Such a dataset, with an accompanying error covariance estimate could be used as input to a climate model to better assess the effects of large volcanic eruptions on the radiative balance of the atmosphere. For much of the latter half of that period, there are (and will be) other satellites instruments capable of measuring SO_2 in the limb and the nadir, in particular high resolution spectrometers with very much enhanced accuracy and precision, that will provide correlative information about the quality of the HIRS/2 SO_2 column retrievals that may be considered in retrospective terms. There is also a break in the TOMS record during 1995–1996 that can be filled by HIRS/2 estimates.

It would be highly desirable to extend comparisons from this eruption with TOMS SO_2 in general, comparing a longer record by both instruments for other eruptions, since both provide a unique record of SO_2 potentially spanning many decades. Satellite records of this length for climatologically important trace gases are rare, and would also provide further constraint to volcanic SO_2 emissions in coupled chemistry climate models.

Atmospheric
Measurement
Techniques
Discussions

References

Barton, I., Prata, A., Watterson, I. & Young, S., 'Identification of the Mount Hudson volcanic cloud over SE Australia', Geophys. Res. Lett. 19, 1211–1214, 1992.

5 Bovensmann, H., Burrows, J. P., Buchwitz, M., Frerick, J., Noel, S., Rozanov, V. V., Chance, K. V. and Goede, A. P. H., 'SCIAMACHY: Mission Objectives and Measurement Modes', J. Atmos. Sci. 56, 127–150, 1999.

Carn, S., Strow, L., Souza-Machado, S. D., Edmonds, Y. and Hannon, S., 'Quantifying tropospheric volcanic emissions with AIRS; the 2002 eruption of Mt. Etna (Italy)', Geophys. Res. Lett. 32, L02301, 2005.

10

Carn, S. A., Clarisse, L., and Prata, A., J.,. "Multi-decadal satellite measurements of global volcanic degassing." Journal of Volcanology and Geothermal Research 311, 99-134, 2016

Chahine, M. T., Pagano, T. S., Aumann, H. H. et al., 'AIRS: Improving weather forecasting and providing new data on 15 greenhouse gases', Bull. Am. Meteorol. Soc 87(7), 911–926, 2006.

Campion, R., Salerno, G., Coheur, P.-F., Hurtmans, D., Clarisse, L., Kazahaya, K., Burton, M., Caltabiano, T., Clerbaux, C. and Bernard, A., 'Measuring volcanic degassing of SO_2 in the lower troposphere with ASTER band ratios', J. Volcanol. Geoth. Res. 194, 42–54, 2010.

20

Clerbaux, C., Coheur, P.-F., Clarisse, L., Hadji-Lazaro, J., Hurtmans, D., Turquety, S., Bowman, K., Worden, H. and Carn, S. A., 'Measurements of SO_2 profiles in volcanic plumes from the NASA Tropospheric Emission Spectrometer (TES)', Geophys. Res. Lett 25, L22807, 2008.

25 Clerbaux, C., Coheur, P.-F., Hurtmans, D., Barret, B., Carleer, M., Colin, R., Semeniuk, K., McConnell, J. C., Boone, C. and Bernath, P., 'Carbon monoxide distribution from the ACE-FTS solar occultation measurements', Geophys. Res. Lett. 32, L16S01, 2005.

Coheur, P.-F., Barret, B., Turquety, S., Hurtmans, D., Hadji-Lazaro, J. and Clerbaux, C., 'Retrieval and characterization of 30 ozone vertical profiles from a thermal infrared nadir sounder', J. Geophys. Res. 110, D24303, 2005.

Constantine, E., Bluth, G. & Rose, W, 'TOMS and AVHRR observations of drifting volcanic clouds from the August 1991 eruptions of Cerro Hudson', Remote Sensing of Active Volcanism, AGU Geophysical monograph 116, 45–64, 2000.

Dee, D. P., Uppala, S. M., Simmons, A. J., Berrisford, P., Poli, P., Kobayashi, S., Andrae, U., Balmaseda, M. A., Balsamo, G., Bauer, P., Bechtold, P., Beljaars, A. C. M., van de Berg, L., Bidlot, J., Bormann, N., Delsol, C., Dragani, R., Fuentes, M., Geer, A. J., Haimberger, L., Healy, S. B., Hersbach, H., Hólm, E. V., Isaksen, L., Kållberg, P., Köhler, M., Matricardi, M.,

5   McNally, A. P., Monge-Sanz, B. M., Morcrette, J.-J., Park, B.-K., Peubey, C., de Rosnay, P., Tavolato, C., Thépaut, J.-N. and Vitart, F. (2011), The ERA-Interim reanalysis: configuration and performance of the data assimilation system. Q.J.R. Meteorol. Soc., 137: 553–597. doi:10.1002/qj.828

Dudhia, A. (2002), 'RFM Software User's Manual'. Issue 4.2, http://www.atm.ox.ac.uk/RFM/sum.html.

10

ECMWF, 'An improved general fast radiative transfer model for the assimilation of radiance observations.'. ECMWF Technical Memo No. 345, 2001.

Gottwald, M., Bovensmann, H., Lichtenberg, G., Noel, S., von Bargen, A., Slijkhuis, A., Piters, A., Hoogeveen, R., von

15   Savigny, C., Buchwitz, M., Kokhanovsky, A., Richter, A., Rozanov, A., Holzer-Popp, T., Bramstedt, K., Lambert, J.-C., Skupin, J., Wittrock, F., Schrijver, H. and Burrows, J., SCIAMACHY, Monitoring the Changing Earth's Atmosphere, DLR, 2006.

Guo, S., Bluth, G., Rose, W., Watson, I. and Prata, A., 'Re-evaluation of SO_2 release of 15th June 1991 Pinatubo eruption

20   using ultraviolet and infrared satellite sensors', Geochem Geophys Geosys 5(4), Q04001, 2004.

Hofmann, D., Oltmans, S., Harriss, J., Solomon, S., Dreshler, T. and Johnson, B., 'Observation and possible causes of new ozone depletion in Antarctica', Nature 359, 283–287, 1992.

25   Eisinger, M. and Burrows, J., 'Tropospheric sulfur dioxide observed by the ERS-2 GOME instrument', Geophys. Res. Lett. 25, 41774180, 1998.

JPL, 'Mission and Spacecraft Library (NOAA)'. http://samadhi.jpl.nasa.gov/msl/QuickLooks/tirosnQL.html, 2003.

30   Karagulian, F., Clarisse, L., Clerbaux, C., Prata, A., Hurtmans, D. and Coheur, P., 'Detection of volcanic SO_2, ash, and H_2SO_4 using the Infrared Atmospheric Sounding Interferometer (IASI)', J. Geophys. Res. 115, D00L02, 2010.

Kearney, C. and Watson, I., 'Correcting satellite-based infrared sulfur dioxide retrievals for the presence of silicate ash', J. Geophys. Res.114, D22208, 2009.

Atmospheric
Measurement
Techniques
Discussions

Open Access

EGU

Kerr, J., McElroy, C. and Olafson, R., 'Measurements of ozone with the Brewer ozone spectrophotometer', Proc. Int. Ozone Symp. 1, 74–79, 1980.

5   Khokhar, M., Frankenberg, C., Roozendael, M. V., Beirle, S., Kuhl, S., Richter, A., Platt, U. and Wagner, T., 'Satellite observations of atmospheric SO_2 from volcanic eruptions during the time-period of 1996-2002', Adv. Space. Res. 36, 879–887, 2005.

Krotkov, N. A., Schoeberl, M. R., Morris, G. A., Carn, S., and Yang, K., 'Dispersion and lifetime of the SO_2 cloud from the

10   August 2008 Kasatochi eruption', J. Geophys. Res. 115, D00L20, 2010.

Krueger, A., 'Sighting of El Chichón sulphur dioxide clouds with the Nimbus 7 Total Ozone Mapping Spectrometer', Science 220, 1377–1378, 1983.

15   Krueger, A., Walter, L., Bhartia, P., Schnetzler, C., Krotkov, N., I.Sprod and Bluth, G., 'Volcanic sulphur dioxide measurements from the Total Ozone Mapping Spectrometer (TOMS) instruments', J. Geophys. Res.100, 14057–14076, 1995.

Krueger, A., Krotkov, N. and Carn, S., 'El chichón: The genesis of volcanic sulphur dioxide monitoring from space', J.

20   Volcanol. Geoth. Res., 2007.

Lee, C., Richter, A., Weber, M. and Burrows, J. P., 'SO_2 retrieval from SCIAMACHY using the weighting function DOAS (WFDOAS) technique: comparison with standard DOAS retrieval', Atmos. Chem. Phys. 8, 61376145, 2008.

25   Matricardi, M., The generation of RTTOV regression coefficients for IASI and AIRS using a new profile training set and a new line-by-line database, Technical report, ECMWF. Technical Memorandum 564, 2008.

Matricardi, M., 'A principal component based version of the RTTOV fast radiative transfer model', Q. J. R. Meteorol. Soc. 136 Part A, 1823– 1835, 2010.

30

Miles, G., Grainger, R. and Highwood, E., 'The significance of volcanic eruption strength and frequency for climate', Q. J. Roy. Meteor. Soc. 130, 2361–2376, 2004.

Pieri, D. and Abrams, M., 'ASTER watches the world's volcanoes: a new paradigm for volcanological observations from orbit', J. Volcano. Geotherm. Res. 135, 13–28, 2004.

Poulsen, C., Watts, P., Thomas, G., Sayer, A., Siddans, R., Grainger, R., Lawrence, B., Campmany, E., Dean, S. and Arnold, C., 'Cloud retrievals from satellite data using optimal estimation, evaluation and application to ATSR', J. Atmos. Meas. Tech., 2012.

Prata, A., Rose, W., Self, S. and O'Brien, D., Volcanism and the Earth's Atmosphere, Geophysical Monograph Series, ed. A. Robock and C. Oppenheimer, Vol. 139, American Geophysical Union, Washington, DC, chapter Global, long-term sulphur dioxide measurements from TOVS data: a new tool for studying explosive volcanism and climate, pp. 75–92, 2003.

Prata, A. and Bernado, C., 'Retrieval of volcanic SO_2 column abundance from Atmospheric Infrared Sounder data', J. Geophys. Res. 112, D20204, 2007.

Prata, A. and Kerkmann, J., 'Simultaneous retrieval of volcanic ash and SO_2 using MSG-SEVIRI measurements', Geophys. Res. Lett. 34, L05813, 2007.

Prata, A., Gangale, G., L.Clarisse and Karagulian, F., 'Ash and sulphur dioxide in the 2008 eruptions of Okmok and Kasatochi: Insights from high spectral resolution satellite measurements', J. Geophys. Res. 115, D00L18, 2010.

Read, W., Froidevaux, L. and Waters, J. W., 'Microwave limb sounder measurement of stratospheric SO_2 from the Mt. Pinatubo volcano', Geophys. Res. Lett. 20, 12991302, 1993.

Read, W., Froidvaux, L., Santee, M. and Livesey, N., 'Observations of volcanic SO_2 and HCl from Aura MLS'. American Geophysical Union, Fall Meeting 2009, abstract number V24B-03, 2009.

Saunders, R., Matricardi, M. and Brunel, P., 'An improved fast radiative transfer model for assimilation of satellite radiance observations', Q. J. R. Meteorol. Soc. 125, 1407–1425, 1999.

Siddans, R., 'Fast transmittance modelling of the MSG and MTG solar channels for cloud retrievals - Final Report, Technical report', STFC. Delivered in response to EUMETSAT RFQ 10/202521, 2011.

Schoeberl, M., Doiron, S., Lait, L., Newman, P. and Krueger, A., 'A simulation of the Cerro Hudson SO_2 cloud', J Geophys Res, 98, 2949–2955, 1993.

5

10

15

20

25

30

Smith, W. L., Woolf, H. M, Hayden, C. M., Wark, D., and McMillin, L. M., The TIROS-N operational vertical sounder,Bull. Amer. Meteorol. Soc., 60, 1177-1187, 1979.

5   N. Theys, I. De Smedt, H. Yu, T. Danckaert, J. van Gent, C. Hörmann, T. Wagner, P. Hedelt, H. Bauer, F. Romahn, M. Pedergnana, D. Loyola, and M. Van Roozendael
Atmos. Meas. Tech. Discuss., doi:10.5194/amt-2016-309, 2016

Thomas, H., Watson, I., Kearnet, C., Carn, S., Murray, S., 'A multi-sensor comparison of sulphur dioxide emissions from the
10 2005 eruption of Sierra Negra volcano, Galapagos Islands', Remote Sensing of Environment, 113, 1331-1342.

Thomas, H. E. and Prata, A. J.: Sulphur dioxide as a volcanic ash proxy during the April–May 2010 eruption of Eyjafjallajökull Volcano, Iceland, Atmos. Chem. Phys., 11, 6871-6880, doi:10.5194/acp-11-6871-2011, 2011.

15 Watson, I., Realmuto, V., Rose, W., Prata, A., Bluth, G., Gu, Y., Bader, C. and Yu, T., 'Thermal infrared remote sensing of volcanic emissions using the moderate resolution imaging spectroradiometer', J. Volcanol. Geoth. Res. 135, 75 89, 2004.

Yang, K., Krotkov, N., Krueger, A., Carn, S., Bhartia, P. and Levelt, P., 'Retrieval of large volcanic SO_2 columns from the Aura Ozone Monitoring Instrument: Comparison and limitations', J. Geophys. Res. 112, D24S43, 2007.

20

Yang, K., Dickerson, R., Carn, S., Ge, C. and Wang, J., 'First observations of SO_2 from the satellite Suomi NPP OMPS: Widespread air pollution events over China', Geophys. Res. Lett. Vol. 40, 4957–4962, doi:10.1002/grl.50952, 2013.
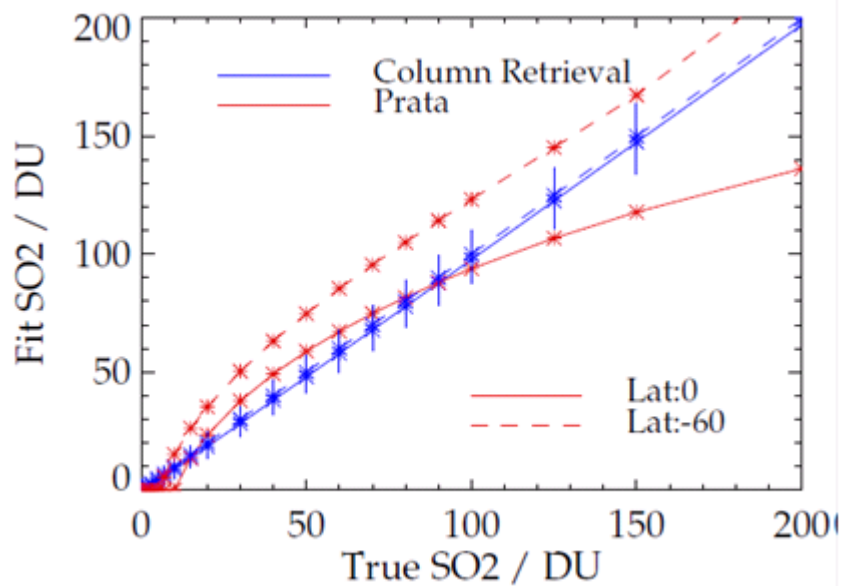
Figure 1: Retrievals based on simulations by a line-by-line model (RFM). These simulations use temperature and water vapour from a cloud-free ECMWF ERA-Interim atmosphere on 15th August 1991, for a grid box centred at 0°E and both 0°N and -60°N and 0°E. The vertical bars show the retrieved error for the column retrieval.
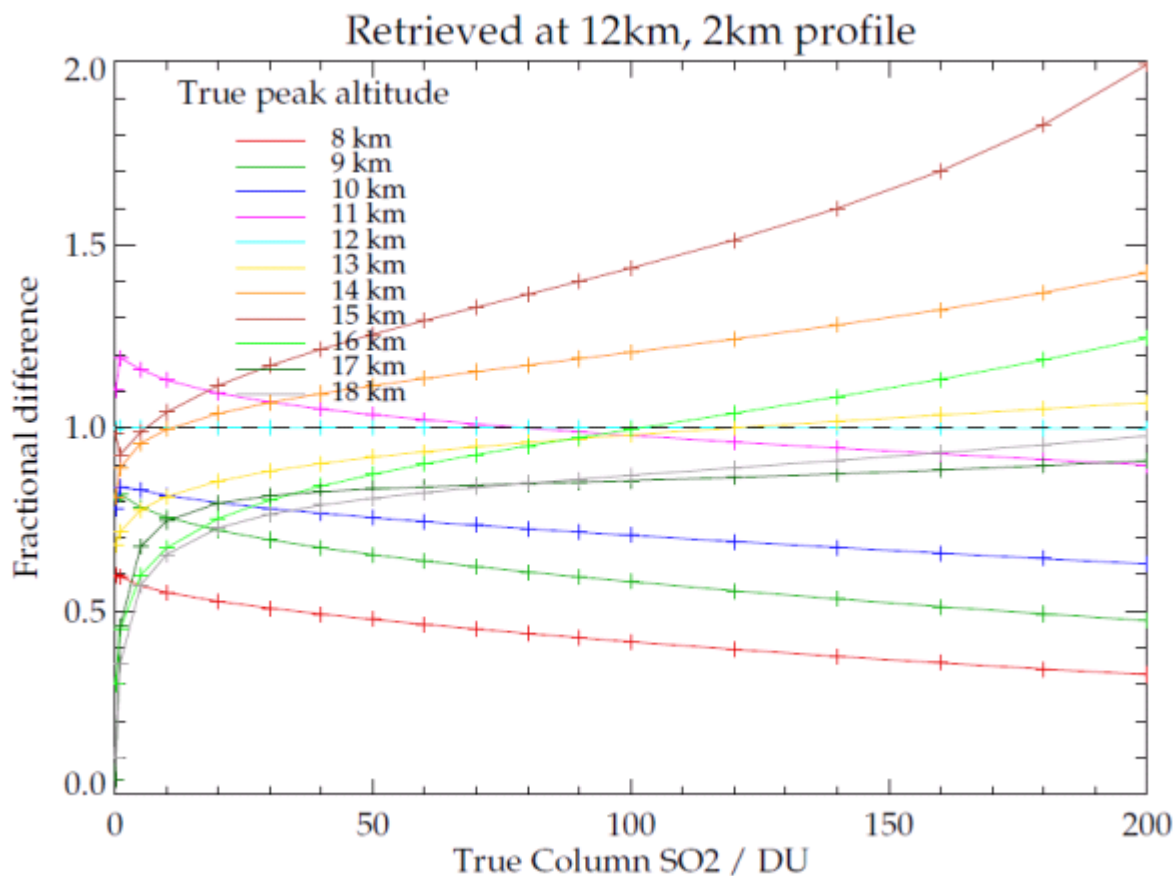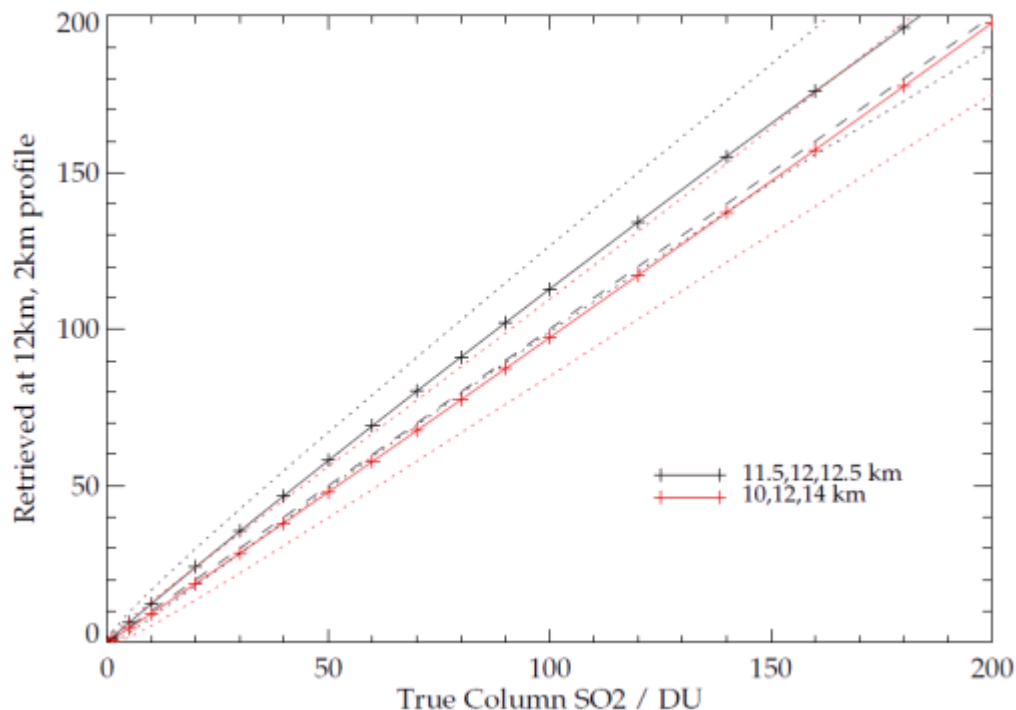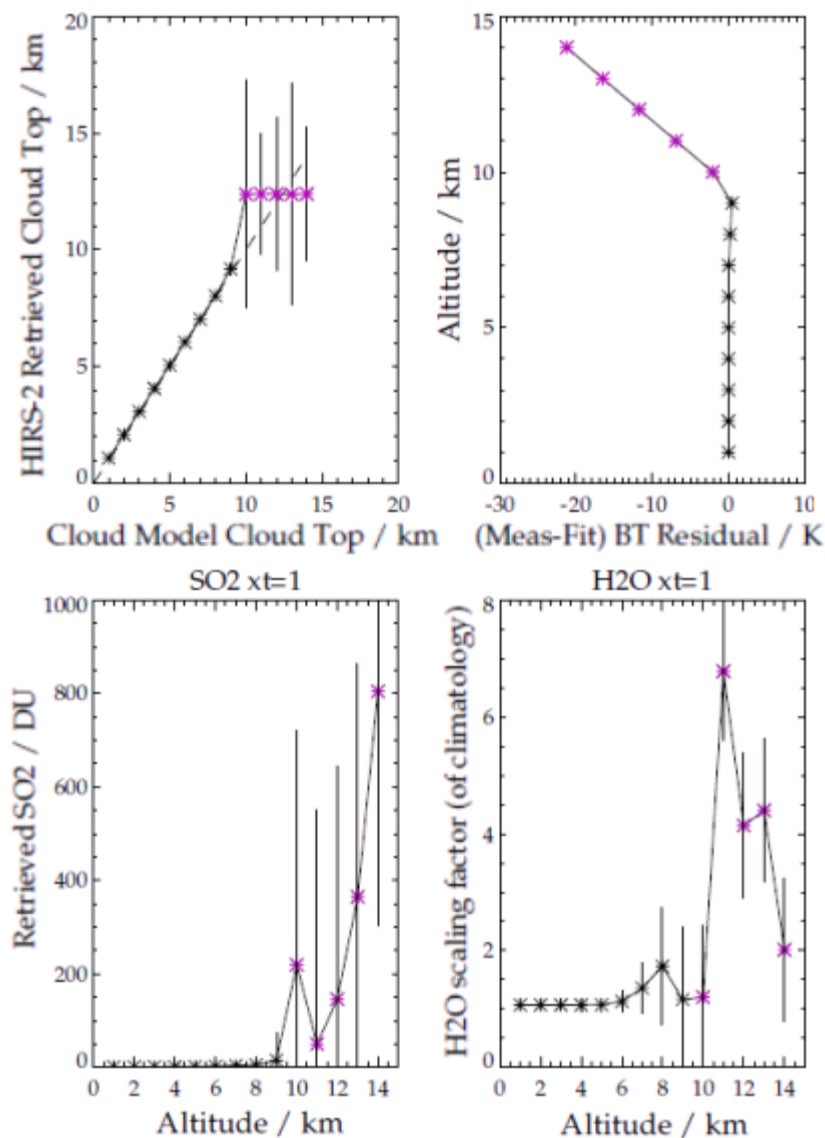
5

Figure 2: A 2 km thick triangular profile centred at 12 km is used to simulate measurements. The profile is then used in a retrieval with the retrieved height assigned to a range of altitudes. The coloured lines indicate the fractional difference to the case when the retrieval used the correct altitude of 12 km.

5

Atmospheric
Measurement
Techniques
Discussions

Open Access

EGU

Figure 3: The black line indicates how columns from 0.1-200 DU are retrieved on a fixed grid with a scalable triangular profile with base, mid-point and top at 11, 12, 13 km respectively, when the true profile shape is given by a triangular profile at 11.5, 12, 13 km, effectively over-estimating the thickness of the plume. The red line shows the equivalent result for an underestimate of the plume thickness, the real profile given by 10, 12, 14 km. The dotted lines show the bounds of retrieved error in each case. The dashed line is x=y shown for clarity.

5

Figure 4. The top left plot shows retrieved cloud top height as a function of 'true' cloud top height as simulated by the cloud model. Black symbols indicate that the retrieval converged and purple indicates that it did not. The top right plot is of the fit residual (measurement minus fit) in the 11.1 µm channel. The bottom left plot shows the retrieved SO_2 as a function of the cloud top height in the cloud model, and the bottom right the equivalent for the water vapour scaling factor.
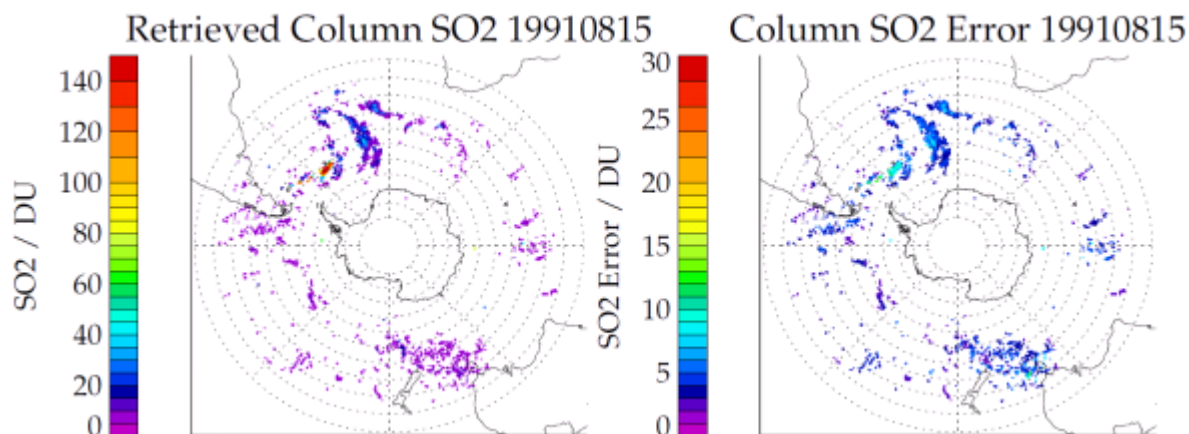
Atmospheric
Measurement
Techniques
Discussions

Figure 5: Retrieved SO$_2$ columns for 15th August 1991, and retrieved error for orbits that day. Erupted SO$_2$ from the start of the eruptive phase (from 8th August 1991) is evident ahead of the larger plume emitted on 15th August. Data are screened at the 2-sigma level (5.4 DU).
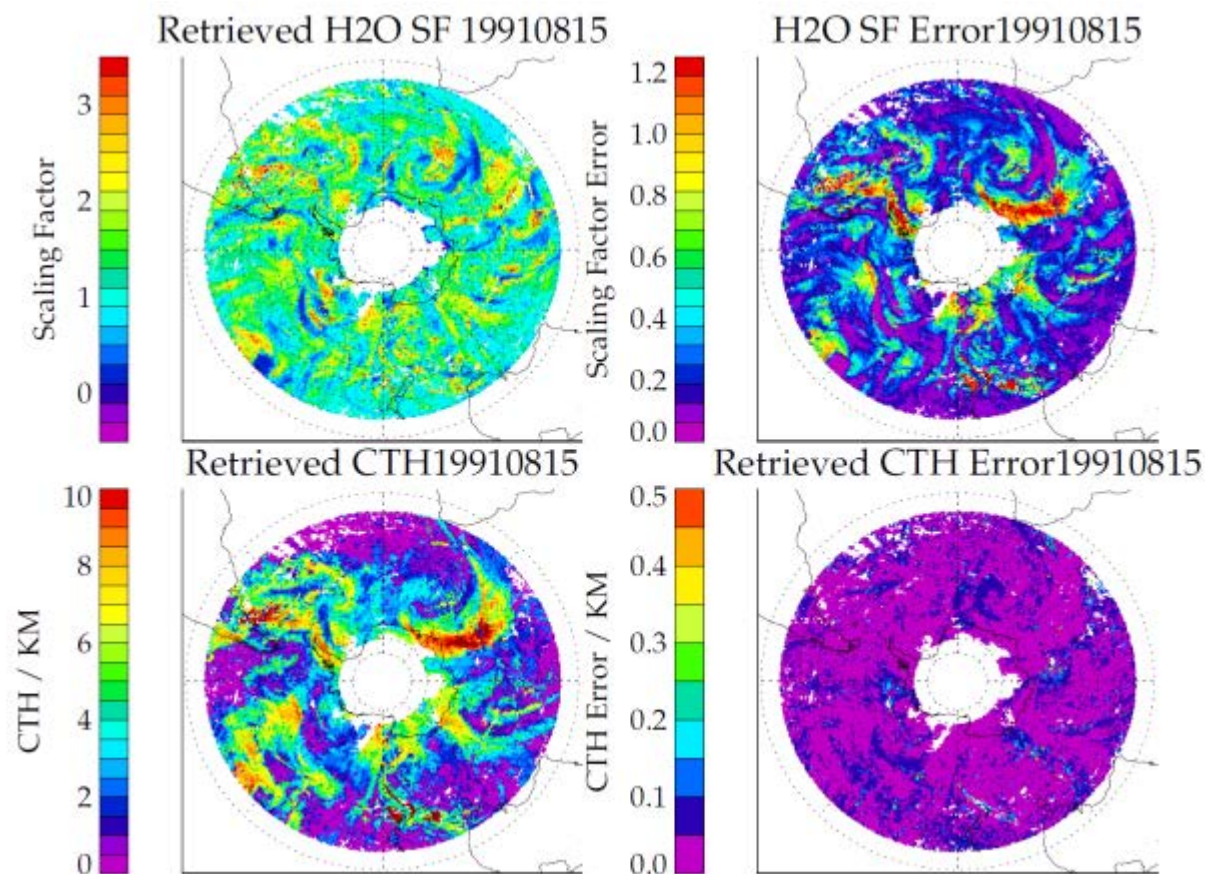
5

Figure 6: The top left and top right show the retrieved water vapour scaling factor and its error from the column retrieval. The bottom left and right the equivalent for the retrieved cloud top height.
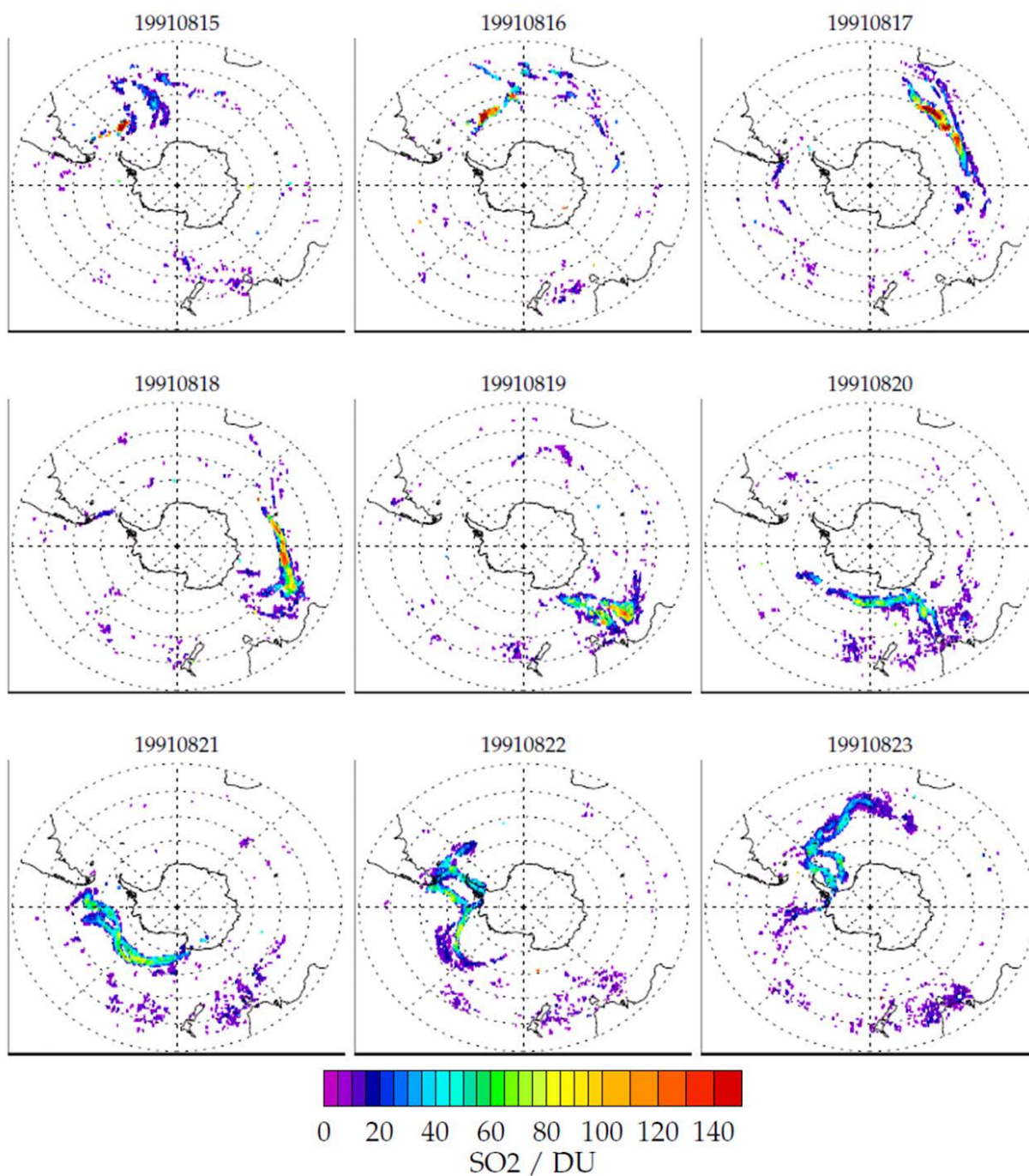
Atmospheric
Measurement
Techniques
Discussions

Figure 7: Progression of main erupted plume from 15th August 1991, using all orbits (day and night) from HIRS/2 NOAA11. The eruption began with smaller amounts emitted from 8th August, which are apparent on 15th and disassociated from the main plume. The plume's transport between observations is evident, particularly from 21st August, where it is captured multiple times by multiple swaths. Data have been screened at the 3-sigma level (8.1 DU) for clarity of the main plume.
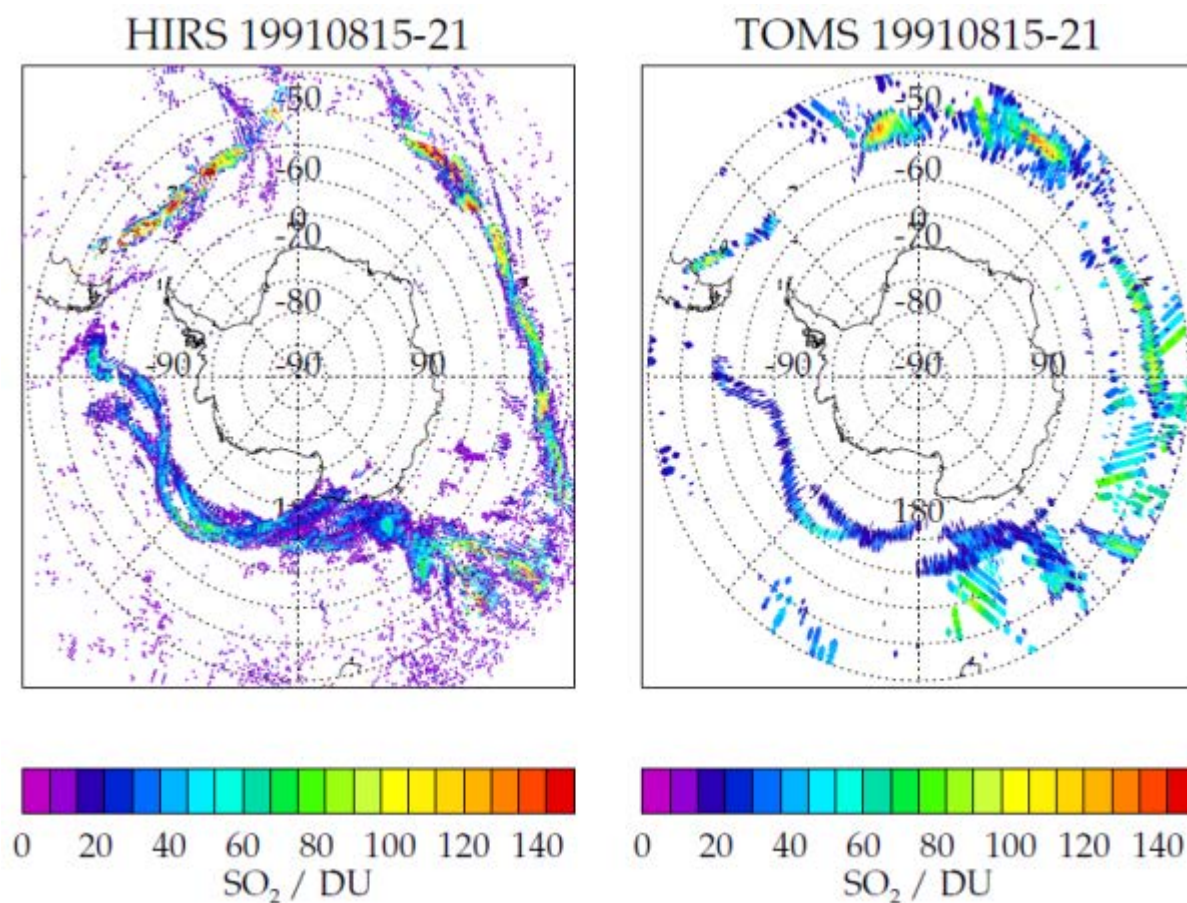
5

Figure 8: Seven day composite of retrieved SO2 from 15-21st August 1991. For clarity in comparison, TOMS data are screened to have a minimum value of 15 DU and HIRS/2 data uses 3 sigma (7.1 DU)
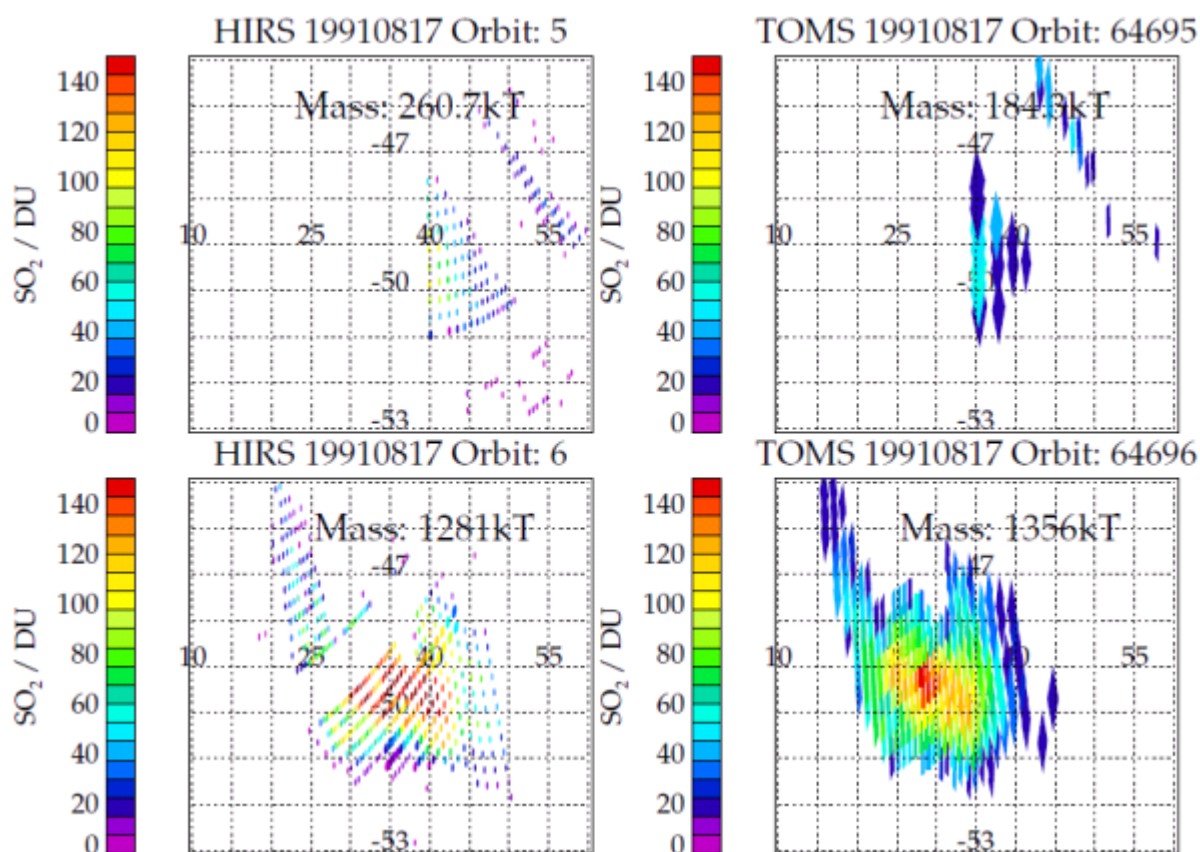
Figure 9: The main Hudson plume on 17th August 1991 as observed in orbits 5 and 6 by HIRS/2 and 64695 and 64696 by TOMS, two days after the main paroxysmal eruption that occurred on 15th August. Four scan lines in the HIRS/2 panels are missing due to routine a calibration phase in which no data are provided. HIRS and TOMS data are both screened at the quality level of 2 -
5 **sigma level (5.4. DU and 15 DU respectively).**

Table 1. Instruments (many of which were flown aboard several different platforms which are not listed) that have been used to measure volcanic SO₂ in the atmosphere.

Instrument name	Viewing geometry, spectral region	Period of operation	Relevant reference
TOMS, TOMS-like instruments (e.g. SBUV/2)	Nadir, UV	1979+	Krueger (1983), Kerr et al. (1980); Krueger et al., (1995, 2007); Guo et al. (2004)
HIRS/2	Nadir, IR	1979+	Prata et al., 2003

Atmospheric
Measurement
Techniques
Discussions

MLS	Limb, IR	1991+	Read et al., (1993, 2009)
GOME, GOME-2	Nadir, UV-vis	1995+	Eisinger & Burrows (1998); Khokhar et al. (2005); Nowlan et al. (2011); Rix et al. (2011)
ASTER	Nadir, IR imager	1999+	Pieri & Abrams (2004); Campion et al., (2010)
MODIS	Nadir, IR Imager	1999+	Watson et al., (2004)
SCIAMACHY	Nadir/Limb, UV-vis	2002-2012	Bovensmann et al., (1999); Gottwald et al., (2006); Lee et al., (2008)
AIRS	Nadir, IR Spectrometer	2002+	Carn et al., (2005); Chahine et al., (2006); Prata & Bernado (2007); Prata et al. (2010)
TES	Nadir, IR FTS	2004+	(Coheur et al. (2005); Clerbaux et al. (2005, 2008))
SEVIRI	GEO, vis/NIR/IR imager	2005+	Prata & Kerkmann (2007); Thomas & Prata (2011)
IASI	Nadir, IR FTS	2006+	Karagulian et al. (2010)
OMI	Nadir, UV	2006+	Krotkov et al. (2010); Yang et al. (2007)
Suomi NPP OMPS	Nadir/Limb, UV	2011+	Yang et al., (2013)
TROPOMI	Nadir spectrometer UV/vis	2017+	Theys et al., (2016)

Table 2. HIRS/2 Instrument Parameters

Instrument Parameter

Cross-track scan   ± 49.5 ° (± 1125 km) nadir

Number of steps	56
Optical Field Of View	1.25 °
Step angle	1.8 °
Ground resolution IFOV (nadir)	17.4 km diameter
Ground resolution IFOV (end of scan)	58.5 km by 29.9 km
Distance between IFOV's	42 km along track and nadir

Table 3. Total erupted SO$_2$ rounded estimates for Cerro Hudson

Eruptive Phase	TOMS SO$_2$[1]	TOMS SO$_2$[2]	HIRS/2 Prata fit[3]	HIRS/2 OE[4]
8-9th August	700 kT	-	300 kT	500 ± 150 kT
12 August	600 kT	-	400 kT	300 ± 90 kT
15 August	2700 kT	2000 kT	1200 kT	1500 ± 400 kT

[1]Constantine et al. (2000)

[2]This work, based on updated TOMS algorithm, for total mass as observed on 16th August (as region poorly observed on 15th) with consideration of pixel overlap within orbit

[3]After Prata et al. (2003) but data reproduced and sampled as OE HIRS/2 product is herein

[4]This work